# Effect of the concentration distribution on the gaseous deflagration propagation in the case of hydrogen/oxygen mixture

Isabelle Sochet, Philippe Gillard, Florent Guelon

# Effect of the concentration distribution on the gaseous deflagration propagation in the case of $H_2/O_2$ mixture

I. Sochet[+] - P. Gillard[*] - F.Guélon[+]
Laboratoire Energétique Explosions Structures - EA1205 - Université d'Orléans

[+] ENSIB 10 boulevard Lahitolle - 18020 BOURGES cedex France
isabelle.sochet@ensi-bourges.fr – Fax : 33 – 2-48 48 40 40
[*] IUT 63 avenue De Lattre de Tassigny - 18020 BOURGES cedex France

**Abstract**

The investigation of flame propagation accompanying the explosions of unconfined gaseous reactive clouds which are diluted in atmosphere ambient is a fundamental interest in the analysis of industrial risk assessment.
Following the previous work Sochet, Guelon, & Gillard (2002), an experimental study is conducted on a deflagration of a hydrogen/oxygen gaseous cloud which is released in air. The burning velocity is directly or indirectly measured. The flammability limits of the non homogeneous cloud has been as well investigated.

*Key words :* deflagration, explosion, hydrogen, non uniform reactive mixture

**Introduction**

During an explosion, one knows that two modes of explosion are possible: the deflagration and the detonation. However, the deflagration process is that probable during an accidental explosion. Indeed, an analysis of 100 major accidents made by Gujan (1978) over one period going from 1921 to 1977 did not reveal any mode of detonation. The deflagration process study in a context of industrial safety is thus of a capital interest. The choice of an $H_2/O_2$ combustible mixture presents a real interest. Indeed, hydrogen is strongly present in industry and its development as a fuel of the future is very probable following ecological considerations ("clean" combustion), geopolitical considerations (research of an energy independence to the Middle East) and the probable end of the hydrocarbon reserves within one century. Following an industrial accident where there is a gas leakage in surrounding air, the gas cloud obtained is not uniform. However it is known that the presence of concentration gradients in a gas mixture has a strong impact on flame propagation during the combustion of this mixture. It is thus essential to have a better knowledge of the flame propagation in non-uniform mixtures for a better understanding of accidental vapour cloud explosion.
From a theoretical point of view [Cambray, & Deshaies, 1978; Deshaies, & Clavin, 1979; Deshaies, & Leyer, 1980], it appears that the overpressure generated by a divergent spherical unconfined deflagration depends on the flame acceleration. However, flame acceleration depends on the concentration gradient of the gas mixture in which it is propagated. With a security aim, study of pressure profile consecutive to a non-uniform gas cloud deflagration thus represents a first approach for a better comprehension of deflagration process in non-uniform mixture. From an experimental point of view, several studies were undertaken. Most of the work performed with non-uniform mixtures deals with the propagation of flames in directions normal to the gradient (Phillips (1965), Hirano, Suzuki, Mashiko, &.Iwai (1977), Girard, Huneau, Rabasse, & Leyer (1978), Badr & Karim (1984), Karim & Lam (1986), Whitehouse, Greig & Koroll (1996)). Most of this work was performed in closed apparatus, a part from the analysis of Girard et al. 1978 which has been conducted in ambient air. In the latter case, the gradients were obtained with concentric soap bubble containing fuel and oxidizer. A significant work was carried out by Whitehouse, Greig & Koroll (1996) on the combustion of non-uniform mixtures hydrogen-air. The tests were carried out in a vertical cylinder of 10.7 $m^3$ (radius of 1.5 m, height of 5.7 m). The hydrogen gradient was such as the weakest hydrogen concentrations were in the low part of the cylinder and strongest ones in the high part. For an ignition at the top of the cylinder, the differences between combustion pressures of gradient and well-mixed gases are most significant when the average concentration of hydrogen is less than 10%. This limit coincides with the downward propagation limit for hydrogen (mixtures containing between 4% and 9% hydrogen will only propagate in the bouyancy assisted upward direction). In a concentration gradient, even though the average hydrogen concentration was below the downward propagation limit, the local concentration at the igniter position was well above this limit. This allowed a large fraction of the hydrogen to be burned, resulting in higher combustion pressures. For the same reason, the flame velocities and the rising rate of pressure observed in gradients were much higher than in well-mixed gases having similar average

quantities of hydrogen and arrival times of wave pressure were much shorter. For an ignition at the bottom of the cylinder, the combustion pressures were about the same for gradient and well-mixed tests exhibiting average hydrogen contentrations below 14%. Above this value, the gradients produced lower combustion pressures than well-mixed gases having similar quantities of hydrogen. This was attributed to a higher burning fraction in the well-mixed gases. Arrival times of pressure wave were much shorter in the homogeneous mixtures than in the stratified mixtures. Indeed, most of the time to peak pressure in the gradient burn was the time that the flame kernel took to travel from the ignition point to the hydrogen rich mixtures at the top of cylinder.
In this paper, we analyse the pressure wave propagation resulting from a non-uniform gas mixture deflagration, the burning velocity and the flammability limits. The experimental results are given in terms of the diffusion of the gas mixture for different initial charges and different ignition locations. The present investigation is conducted at a small scale. The interest of a small scale experimental analysis is to attain an understanding of the phenomena, to isolate more easily the governing parameters and to reproduce a great number of times the experiments contrary to the tests conducted at large scales.

## Experiments

### *2.1 Experimental setup*

The experimental method used in this study to simulate the diffusion and the explosion of a gas cloud is that of the soap bubble. The complet experimental setup was already presented in a previous paper in case of the detonation process (Sochet, Lamy, & Brossard (2000). The hemispherical charges (aqueous confinement) are formed on a horizontal plate (1.25 × 1.85 m) using metal rings (radius $0.03 < R_0 < 0.08$ m). In this study, the gas mixture used is a stoechiometric hydrogen-oxygen mixture.
The non-uniform clouds are obtained by the rupture of aqueous confinement: the diffusion of the gas mixture in surrounding air can then be carried out and the concentration gradient is directly related to the diffusion time noted by $\Delta t$. In experiments (fig. 1) the aqueous confinement is broken by an electromagnetic striker and the diffusion time (i.e. time between the rupture of aqueous confinement and gas cloud ignition) is fixed by a time delay line and controlled by a stop watch.
The ignition of the gas mixtures is obtained by means of an electric spark. The two brass electrodes are separated from 4 mm (inter-axial distance of 6 mm) and the electric power necessary to obtain the spark is stored in a 2 µF condenser under a voltage of 350 V. The nominal energy then delivered during the ignition is 122.5 mJ. The density of the hydrogen-oxygen gas cloud is lower than that of the air, its diffusion in the surrounding atmosphere is thus ascending. To take specificity into account, an altitude ignition device was thus manufactured (fig. 1). Thus, the ignition of the gas cloud can be carried out at any point of space within the explosion limits. The ignition location is referenced by $R_i$, $Z_i$, where $R_i$ is the radial distance starting from the center of the plate and $Z_i$ the altitude level from the plane surface.
A pressure gage equipment allows to characterize the shock wave generated by the explosion of the gas cloud: five piezoelectric pressure gauges are laid out radially, along the same direction, on the plane surface ($R_c$ = 0.117, 0.191, 0.290, 0.491 and 0.692 m measured starting from the center of the plate). Numerical oscilloscopes allow to visualize and acquire the pressure profiles amplified by the charge amplifiers connected to the sensors.
We use an optical system to measure the flame velocity. It contains an interferential filter at 750 nm with a bandwidth of 10 nm corresponding to an OH band, and holds a focusing lens. This system allows to determine a fast signal (~1µs) at a precise point of the dispersion of the $H_2$/air mixture.

### *2.2. Pressure waves profiles*

The evolution of the pressure induced by the deflagration of a stoechiometric hydrogen-oxygen mixture initially confined in a hemispherical volume of initial radius 0.07 m is represented for various diffusion times of the cloud in the air (fig. 2).

The pressure profiles were recorded by a pressure sensor located to 0.117 m of the center of the explosion. The evolution of the pressure wave according to the diffusion time has been described in a previous paper [Sochet, Guelon, & Gillard, 2002]. In the present study, we will study more precisely a specific phenomenon that has been

observed in the previous paper: the appearance of a second peak in the increasing front of the positive phase of pressure wave.
In this case ($R_0$ = 0.07 m, fig. 2), this secondary peak of overpressure appears in the increasing front of the positive phase for a diffusion time $\Delta t$ of 140 ms. Then, as the diffusion time increases, secondary peak is more detached from the principal peak of overpressure. Thus, between the profile of appearance of this secondary peak ($\Delta t$ = 140 ms) and the signal taken to $\Delta t$ = 220 ms, one notes that the secondary peak moved 3 ms away from the main peak.
This phenomenon is explained by the division of the gas charge in two clouds caused, after a certain time, by the diffusion of the cloud in the surrounding air (mushroom shape cloud). The secondary peak comes from the explosion of the low part of the cloud. Then, when the diffusion time increases, the distance between the two gas charges (high part and low part of the cloud) increases and the secondary peak is detached, then moves away from the principal peak of overpressure (fig. 2).
The overall study of the pressure waves as a function of time of diffusion (profiles not represented), for various initial radius of confinement of the cloud and various ignition location, shows diffusion times where a secondary peak of overpressure is observed. These results are synthesized in the table 1.

The results of the table confirm the division of the initial charge in two fractions related to the diffusion: diffusion time corresponding to the appearance of the secondary peak increases with the initial radius of confinement and no appearance of the secondary peak is noted for an altitude ignition higher than 0.03 m and for a radial ignition higher than 0.03 m ($R_0$ = 0.07 m).

For result analysis, the following terms are defined:

- Reduced radial distance (m.MJ$^{-1/3}$) : $\lambda = \frac{R_c}{\sqrt[3]{E}}$ ;
- Reduced positive impulse (bar.ms. MJ$^{-1/3}$) : $\frac{I+}{\sqrt[3]{E}}$ ;
- Relative positive peak overpressure : $\frac{\Delta P+}{P_0}$ ;
- Reduced arrival time (ms. MJ$^{-1/3}$) : $\frac{t_a}{\sqrt[3]{E}}$ ;
- Adimensional number $\frac{D_c}{R_0}$ who represents ratio of the distance between ignition source and the sensor ($D_c$ ) on the initial radius of confinement ($R_0$). The distance $D_c$ in the case of a radial ignition, is then equal to $R_c$ and, in the case of an altitude ignition to $\sqrt{R_c^2+Z_i^2}$ .

*2.3. Uniform cloud*

**2.3.1. Volume influence**

Relative positive peak overpressure (fig. 3a), reduced positive impulse (fig. 3b) and reduced arrival time (fig. 3c) are plotted versus $R_0$ for various radial distances from the sensor ($R_c$ = 0.117, 0.191, 0.290, 0.491 and 0.692 m).
The curves show that the increase of the initial radius of confinement yields an increase of the relative positive peak overpressure and the reduced positive impulse, and a decrease of the reduced arrival time. Based on the experimental results obtained, it is possible to provide an empirical correlation of each parameter observed according to the radial coordinate $R_c$ (m) and of the initial radius of confinement $R_0$ (m) :

- For relative positive peak overpressure :

$$\frac{\Delta P^+}{P_0} = 0.3885 \times R_c^{-1.180} \times R_0^{1.127} \text{ for } 0.10 \le R_c\,(\text{m}) \le 0.70 \text{ and } 0.04 \le R_0\,(\text{m}) \le 0.08$$

- For reduced positive impulse :

$$\frac{I^+}{\sqrt[3]{E}} = 0.9033 \times R_c^{-1.060} \times R_0^{1.078} \text{ for } 0.10 \le R_c\,(\text{m}) \le 0.70 \text{ and } 0.04 \le R_0\,(\text{m}) \le 0.08$$

- For reduced arrival time :

$$\frac{t_a}{\sqrt[3]{E}} = 0.8941 \times R_c^{1.086} \times R_0^{-1.037} \text{ for } 0.10 \le R_c\,(\text{m}) \le 0.70 \text{ and } 0.04 \le R_0\,(\text{m}) \le 0.08$$

It is significant to note that these correlations were given, and thus are valid only for the radial coordinates ($R_c$) and the initial radius of confinement mentioned.

**2.3.2 Location ignition influence**

**2.3.2.1. Radial ignition**

Relative positive peak overpressure (fig. 4a), reduced positive impulse (fig. 4b) and reduced arrival time (fig. 4c) are presented according to the non-dimensional number $D_c/R_0$ for various radial ignition ($R_i$ = 0.00, 0.01, 0.03, 0.05, 0.07 m, $Z_i$ = 0.00 m).
The observation of the figures shows that the increase of the radial coordinate ignition $R_i$ yields a reduction of the relative positive peak overpressure and of the reduced positive impulse. However, the reduced arrival time does not vary much with the increase of the radial coordinate ignition except for ignition at the periphery of the hemispherical confinement ($R_0$ = 0.07 m) which seems consistent with the explosibility limit of the cloud.
The analysis of the experimental points, enables to associate empirical correlations that show the evolution of relative positive peak overpressure and reduced positive impulse as a function of the non-dimensional number $D_c/R_0$ and ignition radius $R_i$ (m):

- For relative positive peak overpressure :

$$\frac{\Delta P^+}{P_0} = 0.2982 \times e^{-23.96 R_i} \times \left(\frac{D_c}{R_0}\right)^{-0.8544} \text{ for } 0 \le \text{Ri}(\text{m}) \le 0.07 \text{ and } 1.671 \le \frac{D_c}{R_0} \le 9.886$$

- For reduced positive impulse :

$$\frac{I^+}{\sqrt[3]{E}} = 0.7671 \times e^{-12.82 R_i} \times \left(\frac{D_c}{R_0}\right)^{-0.9624} \text{ for } 0 \le \text{Ri}(\text{m}) \le 0.07 \text{ and } 1.671 \le \frac{D_c}{R_0} \le 9.886$$

Keeping away the curve that exhibits the reduced arrival time as a function of the non-dimensional number $D_c/R_0$ for the ignition radial coordinate $R_i$ = 0.07 m, one obtains a simple empirical correlation between the reduced arrival time and the adimensional number $D_c/R_0$ :

$$\frac{t_a}{\sqrt[3]{E}} = 0.8405 \left(\frac{D_c}{R_0}\right)^{1.088} \text{ for } 1.671 \le \frac{D_c}{R_0} \le 9.886$$

*2.3.2.2. Altitude ignition*

The evolution of relative positive peak overpressure (fig. 5a), reduced positive impulse (fig. 5b) and reduced arrival time (fig. 5c) are represented versus the adimensional number $D_c/R_0$ for various altitude ignition ($R_i$ = 0.00 m, $Z_i$ = 0.00, 0.01, 0.03, 0.05, 0.07 m).

The experimental results show two phases for relative positive peak overpressure :

- in the first place we note :

$$\frac{\Delta P^+}{P_0}\ (Z_i = 0.00 \text{ m}) < \frac{\Delta P^+}{P_0}\ (Z_i = 0.01 \text{ m}) < \frac{\Delta P^+}{P_0}\ (Z_i = 0.03 \text{ m})$$

It is explained by an ignition which is more centered on the volume of gas. The ignition source approaches the centre of gravity of the hemispherical cloud. The flame propagation can be carried out either in the all space and or in half space as in the case of the centered ignition ($R_i$ = 0.00 m, $Z_i$ = 0.00 m).

- furthermore we note :

$$\frac{\Delta P^+}{P_0}\ (Z_i = 0.00\ m) > \frac{\Delta P^+}{P_0}\ (Z_i = 0.05\ m) > \frac{\Delta P^+}{P_0}\ (Z_i = 0.07\ m)$$

On the top of the hemispherical charge, the radial distribution of gas becomes less significant and, as in the case of a radial ignition, it is logical that the relative positive peak overpressure decreases compared to a centered ignition ($R_i$ = 0.00 m, $Z_i$ = 0.00 m).

The experimental data related to the reduced positive impulse are less contrasted than those of the relative positive peak overpressure. The values of the reduced positive impulse observed for altitude ignition of 0.00, 0.01 and 0.03 m are nearly identical and one finds a decrease of these values for $Z_i$ = 0.05 et 0.07 m.
Thus, it seems that the centring of the ignition to the gas charge has a significant impact on relative positive peak overpressure as opposite to the reduced positive impulse.

The reduced arrival time versus to the adimensional number $D_c/R_0$ is independent of altitude ignition. As in the case of a radial ignition, the experimental points lead to a simple empirical correlation between the reduced arrival time and the adimensional number $D_c/R_0$ :

$$\frac{t_a}{\sqrt[3]{E}} = 0.7584\left(\frac{D_c}{R_0}\right)^{1.111} \quad \text{for } 1.671 \le \frac{D_c}{R_0} \le 9.936$$

*2.4. Non-uniform cloud*

**2.4.1. Centered ignition**

The evolution of relative positive peak overpressure (fig. 6a), reduced positive impulse (fig. 6b) and reduced arrival time (fig. 6c) are presented as a function of the adimensional number $D_c/R_0$ for a centered ignition of non-uniform (diffusion time $\Delta t$ = 20, 40, 60, 80, 100, 140, 180 and 200 ms).

For diffusion times of 40 and 60 ms, a significant increase in relative positive peak overpressure compared to that obtained in the case of a uniform cloud is noted. This disturbance is probably due to the rupture mode of the soap bubble confinement.
Under these conditions while curve obtained for diffusion times of gas of 40 and 60 ms, one observes a decrease in relative positive peak overpressure as a function of diffusion time. An empirical correlation can be deduced between relative positive peak overpressure, the adimensional number $D_c/R_0$ and the diffusion time $\Delta t$ (ms):

$$\frac{\Delta P^+}{P_0} = 0.2935 \times e^{-0.0042\Delta t} \times \left(\frac{D_c}{R_0}\right)^{-0.8269} \quad \text{for } 1.671 \le \frac{D_c}{R_0} \le 9.886 \text{ and } 0 \le \Delta t(ms) \le 200$$

The reduced positive impulse also decreases with the increase of the diffusion time of gas in surrounding atmosphere. At this point, still neglecting the two unmatched diffusion times, it is possible to define an empirical correlation between the reduced positive impulse, the adimensional number $D_c/R_0$ and the diffusion time $\Delta t$ (ms):

$$\frac{I^+}{\sqrt[3]{E}} = 0.8326 \times e^{-0.0033\Delta t} \times \left(\frac{D_c}{R_0}\right)^{-0.9309} \quad \text{for } 1.671 \le \frac{D_c}{R_0} \le 9.886 \text{ and } 0 \le \Delta t(ms) \le 200$$

The reduced arrival time as a function of the adimensional number $D_c/R_0$ is independent of diffusion time. The examination of the experimental points leads to a simple empirical correlation between the reduced arrival time and the adimensional number $D_c/R_0$:

$$\frac{t_a}{\sqrt[3]{E}} = 0.7166\left(\frac{D_c}{R_0}\right)^{1.153} \quad \text{for } 1.671 \le \frac{D_c}{R_0} \le 9.936$$

*2.4.2. Influence of the ignition location*

*2.4.2.1 Radial ignition*

The experimental curves obtained for a radial ignition of non-uniform cloud (diffusion time $\Delta t$ = 40, 80, 100, 140, 180 and 200 ms) are presented as a function of the adimensional number $D_c/R_0$ for two radial ignitions ($R_i$ = 0.03 and 0.05 m, fig. 7-8). The relative positive peak overpressure ($R_i$ = 0.03 m fig. 7a, $R_i$ = 0.05 m fig. 8a), reduced positive impulse ($R_i$ = 0.03 m Fig. 7b, $R_i$ = 0.05 m Fig. 8b) and reduced arrival time ($R_i$ = 0.03 m fig. 7c, $R_i$ = 0.05 m fig. 8c) are study.
At a radial ignition of 0.03 m, the relative positive peak overpressure and reduced positive impulse do not fluctuate strongly as the diffusion time increase contrary to the study related to the centered ignition of non-uniform cloud. However, one finds the phenomenon observed at $\Delta t$ = 40 ms for a centered ignition and allotted to the impact of the rupture of confinement : a significant increaseof the relative positive peak overpressure and reduced positive impulse compared to those obtained in the case of a uniform cloud.
In the case of a radial ignition of 0.05 m, it is interesting to note that the relative positive peak overpressure is maximum for diffusion time of 140 and 200 ms whereas for these same time the reduced positive impulse is minimum.
The reduced arrival time according to the adimensional number $D_c/R_0$ is independent of the diffusion time of gas in the surrounding air to $\Delta t$ = 140 ms for $R_i$ = 0.03 m, and to $\Delta t$ = 80 ms for $R_i$ = 0.05 m. For these two radial ignitions and within their limits of diffusion time, it is still possible to deduce a simple empirical relation between reduced arrival time and the adimensional number $D_c/R_0$:

- For $R_i$ = 0.03 m : $\frac{t_a}{\sqrt[3]{E}} = 0.8231\left(\frac{D_c}{R_0}\right)^{1.080}$ for $1.671 \le \frac{D_c}{R_0} \le 9.936$ and $\Delta t \le 140$ ms

- For $R_i$ = 0.05 m : $\frac{t_a}{\sqrt[3]{E}} = 0.9285\left(\frac{D_c}{R_0}\right)^{1.010}$ for $1.671 \le \frac{D_c}{R_0} \le 9.936$ and $\Delta t \le 80$ ms

*2.4.2.2 Altitude ignition*

The experimental results obtained for an altitude ignition of non-uniform cloud (diffusion time $\Delta t$ = 20, 40, 60, 80, 100, 140, 180 et 200 ms) are presented as a function of the adimensional number $D_c/R_0$ for two altitude ignitions ($Z_i$ = 0.05 et 0.07 m, fig. 9-10). The relative positive overpressure peaks ($Z_i$ = 0.05 m fig. 9a, $Z_i$ = 0.07 m fig. 10a), reduced positive impulse ($Z_i$ = 0.05 m fig. 9b, $Z_i$ = 0.07 m fig. 10b) and reduced arrival time ($Z_i$ = 0.05 m fig. 9c, $Z_i$ = 0.07 m fig. 10c) are studied.
The curves of relative positive overpressure peak show the existence of the non-uniform cloud envelope that is more favorable to the explosion. This area moves vertically with the diffusion time $\Delta t$ : for $Z_i$ = 0.05 m, relative positive peak overpressure and reaches a maximum when the diffusion time $\Delta t$ is of the order of 60 and 80 ms and for $Z_i$ = 0.07 m, it is maximum to $\Delta t$ = 140 and 180 ms. The importance and dangerosity of the ascending diffusion character of the hydrogen-oxygen stoechiometric mixture in the air then is well highlighted: the safety decreases with the increase of the diffusion time of the cloud in the air if there is a potential risk of altitude ignition of the cloud.
The experimental results for reduced positive impulse (fig. 9b and 10b) are less contrasted than for relative positive peak overpressure, but they follow the same tendency: reduced positive impulse values for $Z_i$ = 0.05 m are maximum to $\Delta t$ = 80 and 60 ms, and, for $Z_i$ = 0.07 m, they are slightly similar and independent of diffusion time.
There still, for the altitude ignition used, that is being the reduced arrival time according to the adimensional number $D_c/R_0$ is independent of the diffusion time of gas in surrounding air. An empirical relation between reduced arrival time of arrival and adimensional number $D_c/R_0$ is then obtained for each altitude ignition:

- For $Z_i$ = 0.05 m : $\frac{t_a}{\sqrt[3]{E}} = 0.7218\left(\frac{D_c}{R_0}\right)^{1.127}$ for $1.671 \le \frac{D_c}{R_0} \le 9.936$

- For $Z_i = 0.07$ m : $\frac{t_a}{\sqrt[3]{E}} = 0.7476\left(\frac{D_c}{R_0}\right)^{1.109}$ for $1.671 \le \frac{D_c}{R_0} \le 9.936$

*2.5 Remark concerning the arrival time*

In the case of the reduced arrival time, we obtained empirical laws which were independent of the ignition location (uniform cloud), and of the diffusion time of the cloud (non-uniform cloud) of the following form:

$$\frac{t_a}{\sqrt[3]{E}} = a \times \left(\frac{D_c}{R_0}\right)^b$$

The values of the coefficients a and b can be compared according to the configuration of the experiment. Table 2 summarizes the various experimental configurations for which an empirical correlation can be obtained, by specifying the values of a and b deduced and the range of validity they are based on.
Data analysis of table 2 enables to deduce a single empirical law making that yields the reduced arrival time as a function of the adimensional number $D_c/R_0$ in the case of a uniform or non-uniform cloud ($0 \le \Delta t\,(ms) \le 200$) ignited in any point of its vertical axis ($R_i = 0.00$ m, $0.00 \le Z_i\,(m) \le 0.07$). It can be in the form:

$$\frac{t_a}{\sqrt[3]{E}} = 0.736 \times \left(\frac{D_c}{R_0}\right)^{1.125} \quad \text{for } 0 \le \Delta t\,(ms) \le 200 \text{ and } R_i = 0.00 \text{ m}, \ 0.00 \le Z_i\,(m) \le 0.07$$

The factor 0.736 has been obtained by carrying out an average of the a values of lines 2, 3, 4 and 5 of table 2. The standard deviation associated to this average represents 2.73 % of this latter.
The exponent value 1.125 has been obtained by carrying out an average of the b values of lines 2, 3, 4 and 5 of table 2. The standard deviation associated to this average represents 1.81 % of this latter.

*2.6 Experimental burning velocity*

The burning velocity D can be calculated in two ways: a direct or an indirect method. The direct method is based on the use of the optical transducer. The burning velocity is then simply given by d/t ratio where d is the optical transducer-ignition distance and t the arrival time of flame front to the optical transducer (fig.11).
The indirect method is based on the analogy of piston proposed by Deshaies, & Clavin (1979). This model consists in splitting the flow field of a deflagration in two zones: incompressible and acoustic. The solution gives the pressure P at the radius R and time t as a function of flame propagation $R_F(t)$, the expansion celerity of flame front and its acceleration. By two successive integrations of the pressure signal, the history of flame is deduced. The burning velocity is then defined by the ratio of the expansion celerity of flame front over the expansion ratio (fig.12). Actually, the real limitations of this model are not known, a priori. However, this model is based on the uniform gaseous cloud. Therefore, we use it only for uniform $H_2/O_2$ mixture (i.e. with no diffusion time delay).

## 3 Burning velocity

*3.1. Uniform gaseous cloud*

The burning velocity D, regarded as constant, of a laminar spherical flame being propagated in a hemispherical uniform gas mixture can be calculated from the fundamental flame velocity and the ratio of expansion (ratio of the density of the burned gases to that of fresh gases) by using the relation: $D = \alpha^{-1} V_F$
For a stoechiometric hydrogen-oxygen mixture, the fundamental flame velocity is of 10.73 $m.s^{-1}$ (Chemkin code), the density of fresh gases is of 0.493 $kg.m^{-3}$ to $T_0 = 298$ K and the density of the burned gases is of 0.0580 $kg.m^{-3}$ to 3076 K. One then obtains a burning velocity D constant of 91.2 $m.s^{-1}$.
The burning velocity measured using the optical transducer, for a uniform cloud ignited in its center, are constant but have a dissymmetry with respect of the axis of measurement : 92.17 $m.s^{-1}$ along to the radial axis and 73.10 $m.s^{-1}$ along to the vertical axis. However, one can notice a good adequacy of the value of the speed as a function of the radial axis with the theoretical value of the burning velocity D constant.

From these results, three conclusions can be drawn:

1. The good agreement between the values of the burning velocities obtained directly or indirectly.
2. The velocity burning in a uniform cloud ignited in its centre (initial of containment of 0.07 m) is constant.
3. The relation ( $D = \alpha^{-1} V_F$ ) provides a good approximation of the velocity burning, but it does not describe the dissymmetry observed in the experiments along the R and Z axes which may be explained by the effect of gravity for the vertical component of the velocity and to roughness of the surface for the radial component velocity.

*3.2. Non-uniform gaseous cloud*

The experimental results concerning the speeds of flame measured in experiments using the optical transducer yield the following remarks

1. For a centered ignition source, the flame accelerates according in the ascending direction of the cloud. The length crossed by the flame inside the fresh gas is more significant along Z (0.12 m) that is along to R (0.025 m): the maximum flame velocity along to R is about 30-40 $m.s^{-1}$ and about 50-60 $m.s^{-1}$ along Z.
2. For a non-centered ignition source in height, the measured radial flame velocity (optical transducer in Z = 0 m, moved along to R) increases by 40 to 70 m/s. The velocity also doubles when it is measured vertically (optical transducer in R = 0.00 m, moved along to Z) between Z = 0.04 m and 0.08 m. Nevertheless, this velocity measurement is about twice smaller than the measured radial flame velocity: $V_Z = 0.5V_R$. Along axis Z, with an ignition source in height ($Z_i$ = 0.04 m), the flame crosses a homogeneous zone. The mixture is poor at the point of ignition, the flame velocity ($V_Z$ remains lower than the velocity obtained in a stoechiometric mixture. $V_R$ is then definitely higher than $V_Z$ because the flame is accelerated by the presence of a gradient of reactivity which, although negative, plays a role similar to that a turbulence zone.

## 4 Flammability limits

In the industrial safety context, we have experimentally investigated the explosion limits of a given non-uniform gas cloud in order to know the real zones of ignition of a cloud which diffused in the air. It is a capital interest in this context. For a fixed ignition (centered, radial and in height), we investigated the time of diffusion corresponding to the point where an ignition of the cloud becomes impossible (fig. 13-15).
Taking into account the operating conditions, it is significant to note that the explosion limits measured in these experiments can vary. In order to express the results we systematically defined an explosion limit with a probability equals to 0 and a limit of inflammability with a probability equals to 1. Beyond the first limit, the ignition of the cloud is impossible, below the second one it systematic and between these two, it is random.
The observation of the temporal explosion limits yields the following remarks:

1. When the initial radius of confinement increases, the temporal explosion limits increase. The larger the initial radius of confinement, the greater amount of gas located around source of ignition seems to stagnate. Therefore, more time is required to reach the lower concentration limits hydrogen of the explosion of hydrogen (4%).
2. In the case of an ignition source elevation, the temporal explosion limits increases with the height of ignition of the cloud, but it is not the case for a height of ignition lower than 0.05 m. One can suppose a ground effect (roughness of the table of experiments), which could be have an effect on the diffusion of the cloud in the surrounding air.
3. When the radius of ignition increases, the temporal explosion limits decrease.

## 5 Discussion - Conclusion

The present experiments, conducted at laboratory's scale, for uniform and non-uniform $2H_2 + O_2$ mixtures allow to characterize the pressure wave consecutive to the deflagration as a function of the diffusion time and the ignition location.
In uniform mixtures, the analysis of the pressure profiles enables to provide empiric laws on the reduced arrival time, relative positive peak overpressure and the reduced positive impulse according to the sensor location and to the initial radius of the gas load.
In non-uniform mixtures the pressure profiles highlighted the appearance of a secondary peak in the increasing front of the positive phase. This secondary peak is detached from the principal peak of pressure as the diffusion time

increases. For sufficiently long diffusion times, the cloud adopts a mushroom shape. The secondary peak corresponds to a weak primary explosion before the main explosion of the rest of the cloud. This primary explosion can be defined as the explosion of an under-load of very low volume located at the base of mushroom. The division of the initial charge in two fractions is confirmed for centered, eccentred ignition (on R and Z), and is validated as a function of the volume of the initial charge.

The characteristics of pressure profiles (arrival time, positive overpressure, positive impulse) could be expressed in terms of reduced variables according to the diffusion time and the ignition location. An empirical relation between reduced arrival time of pressure wave and adimensional number $Dc/R_0$ is obtained independently of the diffusion time.Concerning the burning velocity the correlation obtained for a uniform gaseous cloud between experiments and numerical results are in a good agreement. Hence, the burning velocity is equal to 94.68 $m.s^{-1}$ by using the optical transducer, is 116.69 $m.s^{-1}$ by applying the piston model (Deshaies, & Leyer 1980), and is 96.2 $m.s^{-1}$ with the modelling.

In case of the non uniform gaseous cloud, the experimental results show that the flame velocity depends on the reactivity gradient, on the components $V_R$ and $V_Z$. The investigation of temporal inflammability limits show that an explosion can be obtained: i) even though the ignition source is not at the center of the explosive cloud ; ii) even though the gaseous mixture is dispersed into surrounding air. Hence, the importance and dangerosity of the ascending character diffusion of the hydrogen-oxygen stoechiometric mixture in the air is well highlighted. The safety decreases as the diffusion time of the cloud in the air increases. There is a potential risk of altitude ignition of the cloud.

The authors are very much aware that this study was carried out at a laboratory scale and should now be extended to large scale tests coupled to a modelling. Furthermore, the empirical relations which are defined versus the diffusion time could be expressed as a function of the evolution of the concentration. This point will be conducted as soon as possible.

**References**


Badr, O., & Karim, G.A (1984), Flame propagation in stratified methane-air mixtures, *J.Fire Sci.2*, 415-426

Cambray, P., & Deshaies, B. (1978). Ecoulement engendré par un piston sphérique : solution analytique approchée, *Acta Astronautica*, vol.5, 611-617.

Deshaies, B., & Clavin, P. (1970). Effets dynamiques engendrés par une flamme sphérique à vitesse constante, *Journal de mécanique*, vol. 18, n°2, 213.

Deshaies, B., & Leyer, J.C. (1980), Flow field induced by unconfined spherical accelerating flames, *Comb. and Flame*, . Vol. 40, 141-153

Gillard P., & Roux M. (2002) Study of the radiation emitted during the combustion of pyrotechnic charges. Part I: Non stationary measurement of the temperature by means of a two-color pyrometer, *Propellants, Explosives, Pyrotechnics* vol. 27, 72-79

Girard, P., Huneau, M., Rabasse, C., & Leyer, J.C. (1978), Flame propagation through unconfined and confined hemispherical stratified gaseous mixtures. *Proc. 17th Symp. on combustion, Combustion Institute*, Combustion Institute, 1247-1255

Gujan, K. (1978). *Unconfined Vapor Cloud Explosions*, Gulf Publishing Company, 1978.

Hirano, H., Suzuki, T., Mashiko, I. & Iwai, K. (1977), Flame propagation through mixtures with concentration gradients. *Proc. 16th Symp. on combustion,* Combustion Institute, 1307-1315

Karim G.A., & Lam, H.T. (1986), Ignition and flame propagation within stratified methane-air formed by convective diffusion, *Proc. 21st Symp. on combustion*., Combustion Institute, 1909-1915

Magnussen, B.F., & Hjertager, B.H. (1976), On mathematical models of turbulent combustion with special emphasis on soot formation and combustion, *Proc. 16th Symp. on combustion*, Combustion Institute, 719-729

Marinov, N.M., Westbrook, C.K. & Pitz, W.J. (1999). Detailed and global chemical kinetics model for hydrogen, Contract No. W-7405-ENG-48, Lawrence Livermore National Laboratory, P.O. Box 808,L –298, Livermore, CA. 94551, USA, 1999.

Phillips, H. (1965), Flame in a buoyant methane layer, *Proc. 10th Symp. On combustion*, Combustion Institute, 1277-1283

Sochet, I., Guelon F., & Gillard, P. (2002). Deflagrations of non-uniform mixtures : A first experimental approach, *Journal of physics*, vol. 12, 7-273, 7-280.

Sochet, I., Lamy T. and Brossard J. (2000), Experimental investigation on the detonability of non-uniform gaseous mixtures, *Journal Shock Waves*, vol. 10, 363, 2000.

Whitehouse, D.R., Greig, D.R., & Koroll G.W (1996). Combustion of stratified hydrogen-air mixtures in the 10.7 $m^3$ Combustion Test Facility Cylinder, *Nuclear Engineering and Design*, 453-462.

**Symbols**

D : burning velocity ($m.s^{-1}$)
$D_c$ : distance between ignition source and the pressure gauge (m)
E : energy released by the explosion of gaseous charge (MJ)
$I^+$ : positive impulse (bar.ms)
$P_0$ : atmospheric pressure (bar)
$R_c$ : distance, on the plane surface, of the pressure gauge from the center of the plate (m)
$R_i$ : radial distance of the ignition location from the center of the plate (m)
$R_0$ : radius of initial charge (m)
$t_a$ : arrival time (ms)
$V_F$ : fundamental flame velocity ($m.s^{-1}$)
$V_R$ : radial flame velocity ($m.s^{-1}$)
$V_Z$ : vertical flame velocity ($m.s^{-1}$)
$Z_i$ : altitude level of the ignition location from the center of the plate (m)
$\Delta P^+$ : positive overpressure (bar)
$\Delta t$ : diffusion time (ms)

| $R_0$ (m)<br><br>$R_i$ = 0.00 m<br>$Z_i$ = 0.00 m | Time delay of diffusion for secondary peak appearance (ms) | $Z_i$ (m)<br><br>$R_i$ = 0.00 m<br>$R_0$ =0.07 m | Time delay of diffusion for secondary peak appearance (ms) | $R_i$ (m)<br><br>$Z_i$ = 0.00 m<br>$R_0$ =0.07 m | Time delay of diffusion for secondary peak appearance (ms) |
|---|---|---|---|---|---|
| 0.04 | 80 | 0.01 | 160 | 0.01 | 160 |
| 0.05 | 120 | 0.02 | 160 | 0.02 | 160 |
| 0.06 | 130 | 0.03 | 220 | 0.03 | 160 |
| 0.07 | 140 | 0.04 | none | 0.04 | none |
| 0.08 | 160 | 0.05 | none | 0.05 | none |
| | | 0.06 | none | 0.06 | none |
| | | 0.07 | none | 0.07 | none |

Table 1: Diffusion time where the appearance of a secondary peak of overpressure is observed for various sizes of initial cloud in centered ignition, and for clouds with a confinement of radius equal to 0.07 m in eccentric ignition.

| **Test parameters** ($R_0$ = 0.07 m) | a | b | Validity range |
|---|---|---|---|
| $0.00 \le R_i(m) \le 0.07$ , $Z_i$ = 0.00 m<br>Uniform cloud ( $\Delta t$ = 0 ms ) | 0.841 | 1.088 | $0.00 \le R_i(m) \le 0.05$ |
| $R_i$ = 0.00 m, $0.00 \le Z_i(m) \le 0.07$<br>Uniform cloud ( $\Delta t$ = 0 ms ) | 0.758 | 1.111 | $0.00 \le Z_i(m) \le 0.07$ |
| $R_i$ = 0.00 m, $Z_i$ = 0.00 m<br>Non-uniform cloud ( $0 \le \Delta t$ (ms) $\le 200$ ) | 0.717 | 1.153 | $0 \le \Delta t$ (ms) $\le 200$ |
| $R_i$ = 0.00 m, $Z_i$ = 0.05 m<br>Non-uniform cloud ( $0 \le \Delta t$ (ms) $\le 200$ ) | 0.722 | 1.127 | $0 \le \Delta t$ (ms) $\le 200$ |
| $R_i$ = 0.00 m, $Z_i$ = 0.07 m<br>Non-uniform cloud ( $0 \le \Delta t$ (ms) $\le 200$ ) | 0.748 | 1.109 | $0 \le \Delta t$ (ms) $\le 200$ |
| $R_i$ = 0.03 m, $Z_i$ = 0.00 m<br>Non-uniform cloud ( $0 \le \Delta t$ (ms) $\le 200$ ) | 0.823 | 1.080 | $0 \le \Delta t$ (ms) $\le 140$ |
| $R_i$ = 0.05 m, $Z_i$ = 0.00 m<br>Non-uniform cloud ( $0 \le \Delta t$ (ms) $\le 200$ ) | 0.929 | 1.010 | $0 \le \Delta t$ (ms) $\le 80$ |

Table 2 : Empiric laws for reduced arrival time.

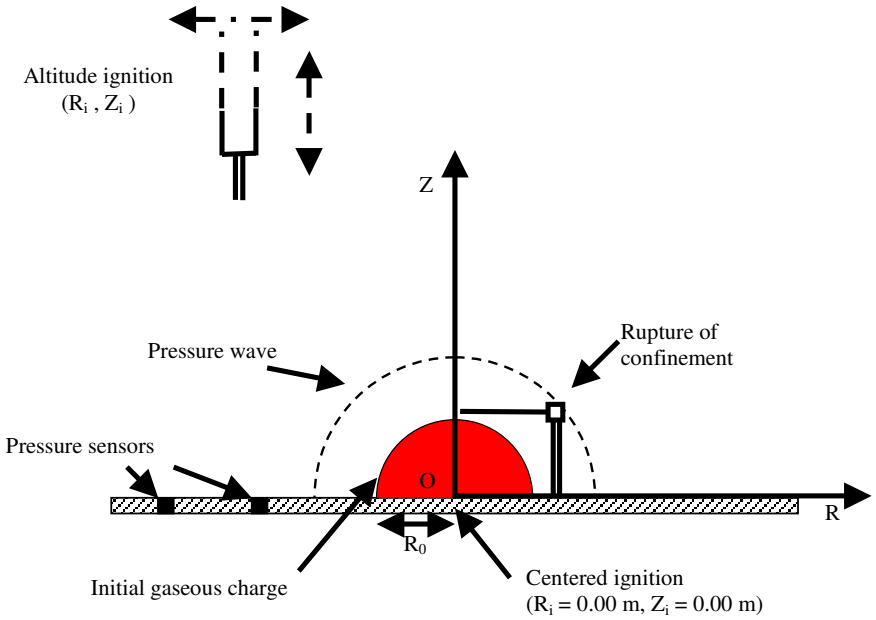


Figure 1: Experimental setup

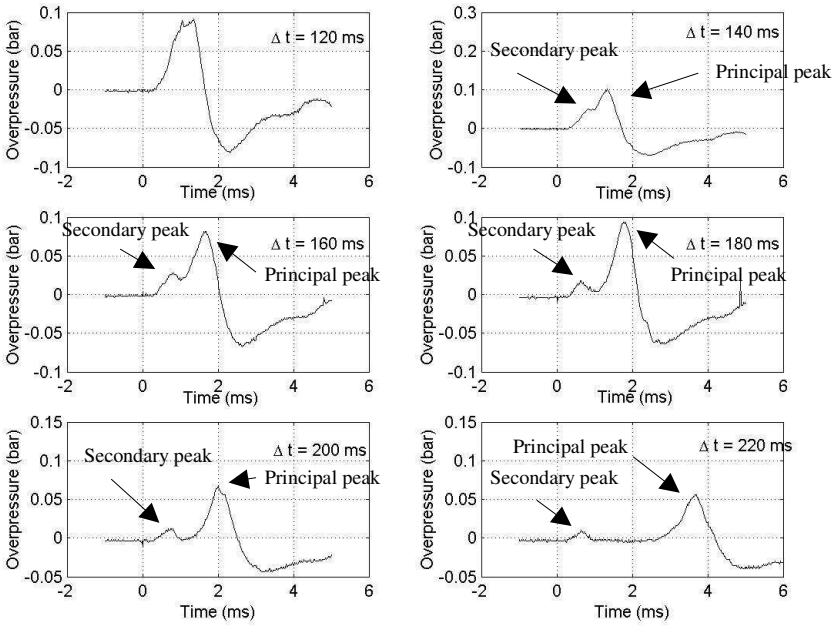


Figure 2: Pressure profile ($R_c$ = 0.117 m) resulting of a $2H_2$+$O_2$ mixture deflagration ($R_0$ = 0.07 m) for different time delay of diffusion Δt. Centered ignition (0, 0).

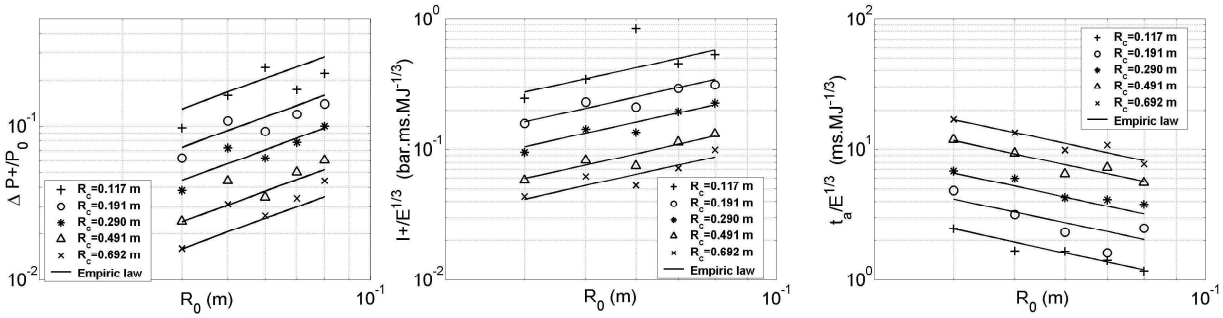


Figure 3 : Uniform mixtures - Relative positive peak overpressure (a), reduced positive impulse (b) and reduced arrival time (c) of pressure wave as a function of the adimensional number $D_c/R_0$ for various initial radius of confinement.

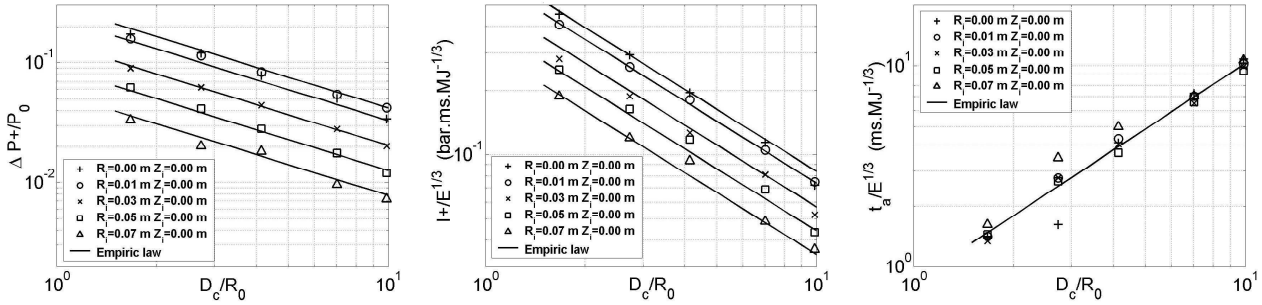


a b c

Figure 4 : Uniform mixtures - Relative positive peak overpressure (a), reduced positive impulse (b) and reduced arrival time (c) of pressure wave as a function of the adimensional number $D_c/R_0$ for various radial ignition. Initial radius of confinement: 0.07 m.

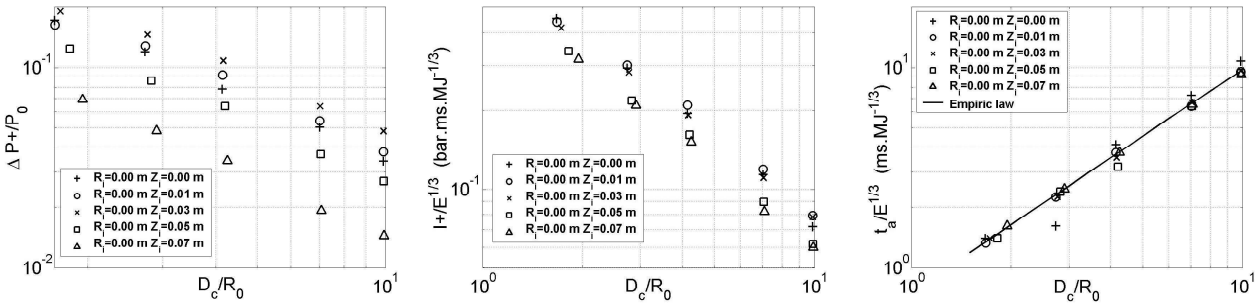


a b c

Figure 5 : Uniform mixtures - Relative positive peak overpressure (a), reduced positive impulse (b) and reduced arrival time (c) of pressure wave as a function of the adimensional number $D_c/R_0$ for various altitude ignition. Initial radius of confinement : 0.07 m

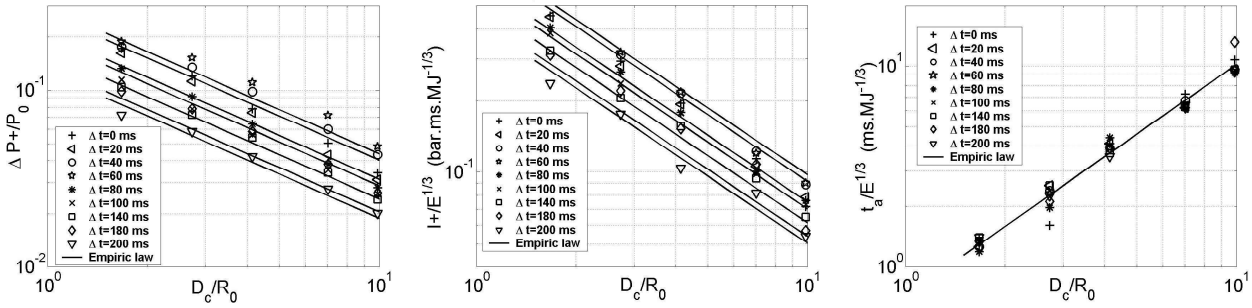


Figure 6: Relative positive peak overpressure (a), reduced positive impulse (b) and reduced arrival time (c) of pressure wave as a function of the adimensional number $D_c/R_0$ for various diffusion time. Initial radius of confinement: 0.07 m**.** Centered ignition (0, 0).

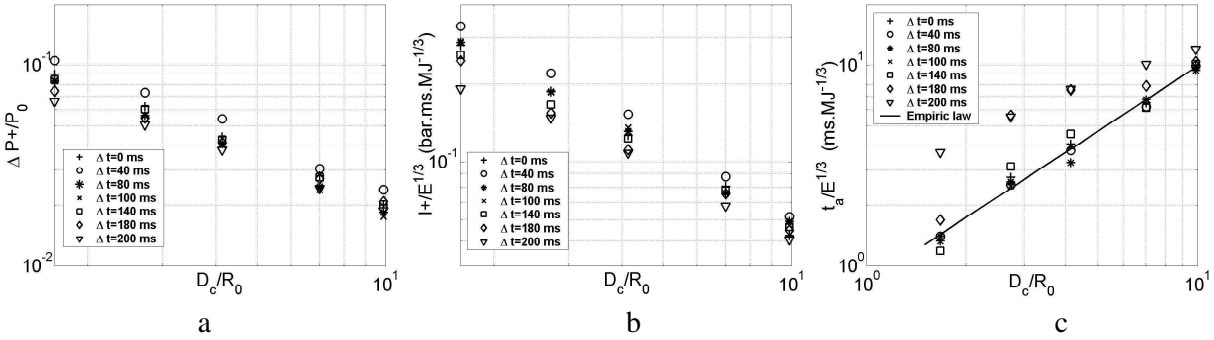


Figure 7 : Relative positive peak overpressure (a), reduced positive impulse (b) and reduced arrival time (c) of pressure wave as a function of the adimensional number $D_c/R_0$ for various diffusion time. Initial radius of confinement : 0.07 m . Radial ignition ($R_i$ = 0.03 m, $Z_i$ = 0.00 m).

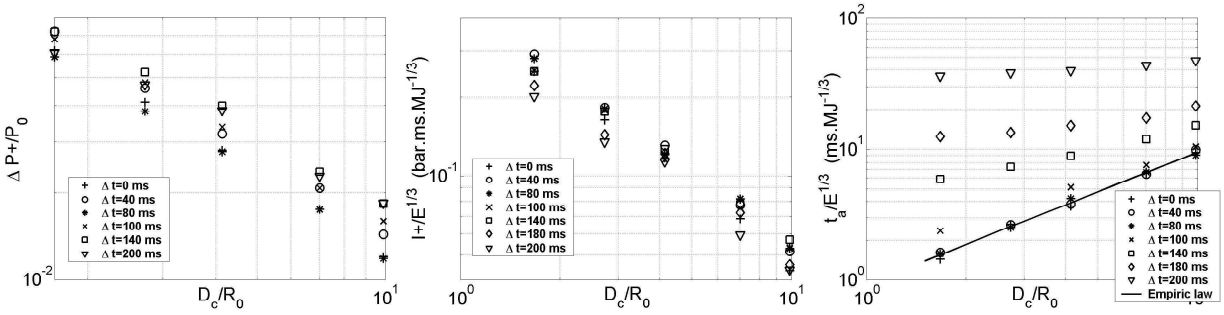


a b c

Figure 8 : Relative positive peak overpressure (a), reduced positive impulse (b) and reduced arrival time (c) of pressure wave as a function of the adimensional number $D_c/R_0$ for various diffusion time. Initial radius of confinement : 0.07 m . Radial ignition ($R_i$ = 0.05 m, $Z_i$ = 0.00 m).

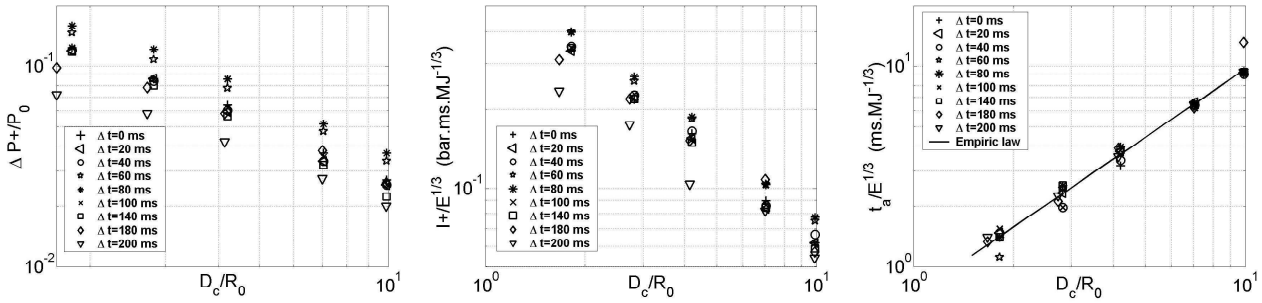


Figure 9 : Relative positive peak overpressure (a), reduced positive impulse (b) and reduced arrival time (c) of pressure wave as a function of the adimensional number $D_c/R_0$ for various diffusion time. Initial radius of confinement : 0.07 m . Altitude ignition ($R_i$ = 0.00 m, $Z_i$ = 0.05 m).

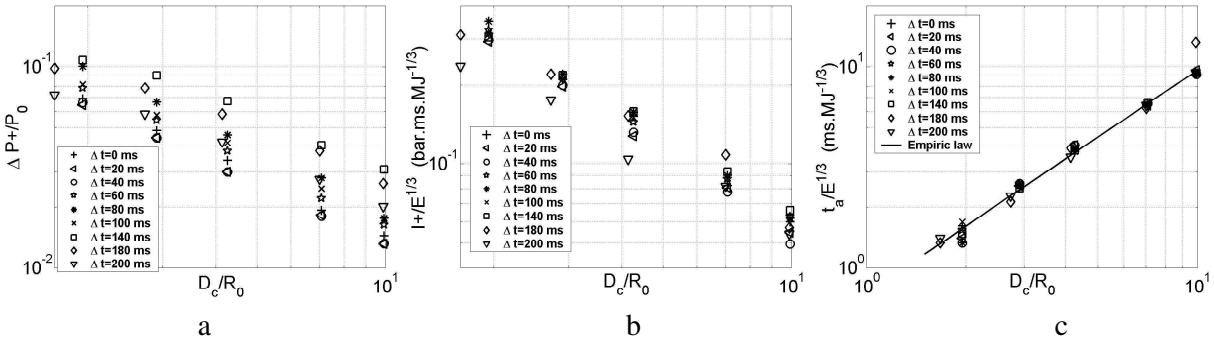


Figure 10 : Relative positive peak overpressure (a), reduced positive impulse (b) and reduced arrival time (c) of pressure wave as a function of the adimensional number $D_c/R_0$ for various diffusion time. Initial radius of confinement: 0.07 m. Altitude ignition ($R_i$ = 0.00 m, $Z_i$ = 0.07 m).

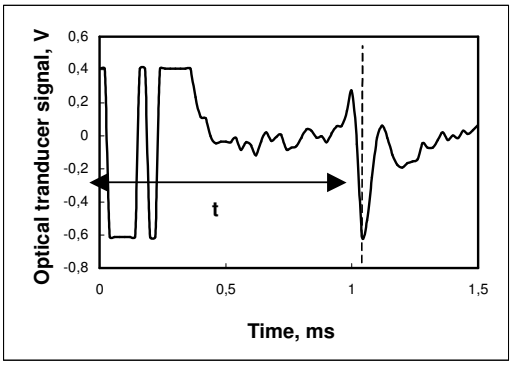

Figure 11: Optical transducer signal versus time

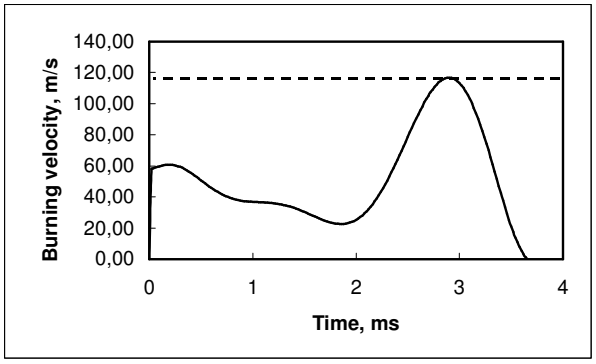

Figure 12: Burning velocity calculated from pressure record (at 0.692 m)- 2 $H_2$+$O_2$ - 1 atm - 298 K

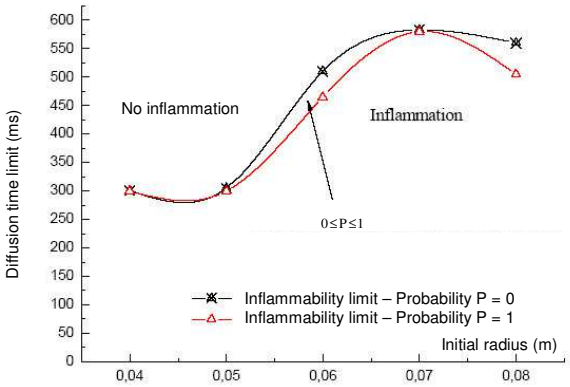


Figure 13 : Experimental temporal explosion limits of a non-uniform hydrogen-oxygen cloud versus the initial radius of confinement. Centered ignition ($R_i$ = 0 m, $Z_i$ = 0 m)

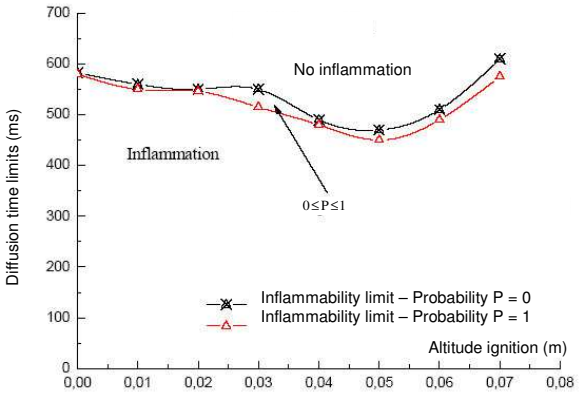


Figure 14 : Experimental temporal explosion limits of a non-uniform hydrogen-oxygen cloud versus the altitude position of ignition source. Decentered ignition ($R_i$ = 0 m, $Z_i$ > 0 m)

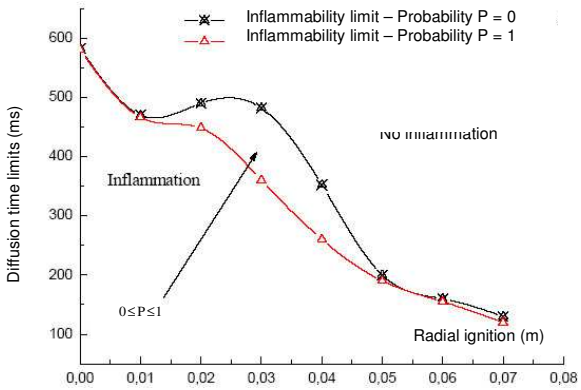


Figure 15 : Experimental temporal explosion limits of a non-uniform hydrogen-oxygen cloud versus the radial position of ignition source. Decentered ignition ($R_i > 0$ m, $Z_i = 0$ m)